DESIGN PRINCIPLES FOR HIGH CURRENT BEAM INJECTION LINES

H. Liu and D. Neuffer, CEBAF, 12000 Jefferson Ave., Newport News, VA 23606, USA

We discuss the design principles for high current injection beam lines having a high degree of beam quality preservation. These principles are applied to designing a high current e-beam injection line delivering 10 MeV e-beams from the injector to an accelerator driving UV FELs, as proposed at CEBAF.

I. INTRODUCTION

A 200 MeV recirculating SRF e-beam accelerator is being designed at CEBAF for driving kW-level industrial UV FELs [1, 2]. This accelerator, like all the FEL drivers, should provide e-beams having the smallest possible emittances. This demands minimization of the emittance growth at all of the stages of beam creation, acceleration and transport. One of the most critical regions is the injection line which transports the e-beams from a CW high current 10 MeV injector [3] to the accelerator.

It is interesting to consider in general how a high current injection beam line should be designed to provide a high degree of beam quality preservation, while providing the required matching conditions into the accelerator. For a non-circulating accelerator, one can minimize the emittance growth in the bending system by minimizing the average beam size [5], and match the beam into the accelerator by adding quadrupoles after the last dipole of the beam bending line. However, this prescription does not apply to a circulating accelerator, since the quads added between the last dipole and the accelerator disturbs the lattice for high-pass accelerated beams [6]. Alternative prescriptions must be sought for the latter case.

II. GENERAL DESIGN PRINCIPLES

The first general principle that an injection line design should follow is symmetry. A symmetric bending system preserves the beam emittance better than an asymmetric bending system, since the symmetry minimizes the aberrations. Also, a symmetric achromatic system is more compact, since an asymmetric system requires more elements and more length to become achromatic.

Secondly, the beam should be bent gently. The bending angle is often limited by the given footprint or space to clear the high-pass accelerated beams from the injected beams. A rule-of-thumb has been given in [7] that the magnitude of the deflection of the injected beam should be less than $3^o \times (W_1/W_0)$, where W_1 and W_0 are the energies of the first orbit and the injected beams respectively. This ratio is generally less than 10, so the maximum magnitude of the deflection of the injected beam should be less than 30^o for a circulating accelerator.

Thirdly, the length of an injection line should be minimized. Therefore, a minimum number of magnets constituting an achromatic system should be used. One can use a single α-magnet [8] or two conventional dipoles with a quad in between to constitute an achromatic bending system. However, for more flexible beam matching and axial bunching, at least three dipoles are needed.

Fourth, the beam line should retain a high degree of flexibility in matching so that neither injector beams nor main accelerator beams are required to meet precise specifications in order to function.

III. EMITTANCE GROWTH

Beam emittance growth in bends has been studied in detail in [9]. The responsible mechanisms were attributed to the anomalous noninertial transverse space-charge force and the normal longitudinal space-charge force. Useful formulas have been given for estimating the emittance growth from these two mechanisms.

In some earlier particle simulations of high current beam transport through an injection line [4], we turned the transverse and axial space charge forces on and off alternatively, and identified the axial space charge force as the cause of the emittance growth. The underlying mechanism is that the momentum of each electron is modified by the axial space charge force, and the beam ends up with a residual dispersion or emittance growth.

We now derive the beam emittance growth in the bending plane defined by the transfer matrix

$$R = \begin{bmatrix} R_{11} & R_{12} & R_{13} \\ R_{21} & R_{22} & R_{23} \\ 0 & 0 & \delta \end{bmatrix}, \qquad (1)$$

where $\delta \approx 1$ is introduced to account for the momentum variation. Due to $\sigma(B) = R\sigma(A)R^T$, we have

$$\begin{aligned}\sigma_{11}(B) &= R_{11}^2\sigma_{11}(A) + 2R_{11}R_{12}\sigma_{12}(A) \\ &\quad + 2R_{11}R_{13}\sigma_{13}(A) + R_{12}^2\sigma_{22}(A) \\ &\quad + 2R_{12}R_{13}\sigma_{23}(A) + R_{13}^2\sigma_{33}(A)\ , \quad (2.1)\end{aligned}$$

$$\begin{aligned}\sigma_{12}(B) &= R_{11}R_{21}\sigma_{11}(A) + (R_{11}R_{22} + R_{12}R_{21})\sigma_{12}(A) \\ &\quad + (R_{11}R_{23} + R_{13}R_{21})\sigma_{13}(A) + R_{12}R_{22}\sigma_{22}(A) \\ &\quad + (R_{12}R_{23} + R_{13}R_{22})\sigma_{23}(A) + R_{13}R_{23}\sigma_{33}(A), \quad (2.2)\end{aligned}$$

$$\begin{aligned}\sigma_{22}(B) &= R_{21}^2\sigma_{11}(A) + 2R_{21}R_{22}\sigma_{12}(A) \\ &\quad + 2R_{23}R_{21}\sigma_{13}(A) + R_{22}^2\sigma_{22}(A) + 2R_{22}R_{23}\sigma_{23}(A) \\ &\quad + R_{23}^2\sigma_{33}(A)\ , \quad (2.3)\end{aligned}$$

$$\sigma_{13}(B) = [R_{11}\sigma_{13}(A) + R_{12}\sigma_{23}(A) + R_{13}\sigma_{33}(A)]\,\delta, \quad (2.4)$$

$$\sigma_{23}(B) = [R_{21}\sigma_{13}(A) + R_{22}\sigma_{23}(A) + R_{23}\sigma_{33}(A)]\,\delta, \quad (2.5)$$

$$\sigma_{33}(B) = \sigma_{33}(A)\,\delta^2\ . \quad (2.6)$$

Then the bending-plane beam emittance at the exit is

$$\varepsilon_x^2(B) = \varepsilon_x^2(A) + \Delta\varepsilon_x^2(B), \text{ where}$$

$$\begin{aligned}\Delta\varepsilon_x^2(B) = {} & [\sigma_{11}(A)\sigma_{33}(A) - \sigma_{13}^2(A)]\, a_1^2 \\ & + [\sigma_{22}(A)\sigma_{33}(A) - \sigma_{23}^2(A)]\, a_2^2 \\ & + 2[\sigma_{11}(A)\sigma_{23}(A) - \sigma_{12}(A)\sigma_{13}(A)]\, a_1 \\ & + 2[\sigma_{12}(A)\sigma_{23}(A) - \sigma_{22}(A)\sigma_{13}(A)]\, a_2 \\ & - 2[\sigma_{13}(A)\sigma_{23}(A) - \sigma_{12}(A)\sigma_{33}(A)]\, a_1 a_2, \quad (3)\end{aligned}$$

where $a_1 = R_{11}R_{23} - R_{13}R_{21}$ and $a_2 = R_{12}R_{23} - R_{13}R_{22}$.

We assume that the bending system is achromatic and symmetric between the first half and the second half, and that the deflection in the second half is in the same sense as the first. Then the transfer matrices for the first half, second half and the overall system are [10],

$$\begin{bmatrix} -1 & 2\alpha_{12}\alpha_{22} & \Delta\eta \\ 0 & -1 & \Delta\eta' \\ 0 & 0 & \delta^2 \end{bmatrix} = \begin{bmatrix} \alpha_{22} & \alpha_{12} & -\alpha_{13}\alpha_{22} \\ -\alpha_{12}^{-1} & 0 & \alpha_{13}\alpha_{12}^{-1} \\ 0 & 0 & \delta \end{bmatrix} \begin{bmatrix} 0 & \alpha_{12} & \alpha_{13} \\ -\alpha_{12}^{-1} & \alpha_{22} & 0 \\ 0 & 0 & \delta \end{bmatrix}, \quad (4)$$

where $\Delta\eta = \alpha_{13}\alpha_{22}(1-\delta)$ and $\Delta\eta' = \alpha_{13}\alpha_{21}(1-\delta)$ are the residual dispersions due to momentum variation. The total emittance growth (normalized) from one end to the other of the bending system is

$$\Delta\varepsilon_{nx} = \eta_c\sqrt{\alpha_{21}^2\sigma_{11}(0) + \alpha_{22}^2\sigma_{22}(0)}\ \Big|\ \sigma_{\gamma\beta}(1)\,\Delta\langle\gamma\beta\rangle\ /\langle\gamma\beta\rangle - (\sigma_{\gamma\beta}(1) - \sigma_{\gamma\beta}(0))\Big|, \quad (5)$$

where η_c is the dispersion at the symmetry plane, $\Delta\langle\gamma\beta\rangle / \langle\gamma\beta\rangle$ is the relative average momentum change, and $\sigma_{\gamma\beta}(1) - \sigma_{\gamma\beta}(0)$ is the absolute change in the normalized rms momentum spread from the entry plane to the symmetry plane. This rms momentum change due to the axial space charge force has been given in [9], and substitution of it into Eq. (5) yields

$$\Delta\varepsilon_{nx} = (3I_pS/8l_bI_A\gamma^2\beta^2)\,(\eta_c/f_x)\,\sigma_x(0), \quad (6)$$

where $I_p = Q\beta c/l_b$ is the peak current, l_b the total bunch length for a uniform distribution or equal to $(2\pi)^{1/2}\sigma_z$ for a Gaussian distribution, I_A = 17 kA, S the half length of the system, $f_x = -1/\alpha_{21}$ is the focal length of the first half of the system, $\sigma_x(0)$ is the initial rms beam size in the x-plane, and we assumed that the beam is nearly parallel at the entry plane, i.e., $\alpha_{21}^2\sigma_{11}(0) >> \alpha_{22}^2\sigma_{22}(0)$. This equation shows the parametric dependence of the emittance growth upon various beam parameters as well as the injection line parameters.

IV. MAGNETIC BUNCHING

Axial bunching occurs if the bending system is non-isochronous. The bunching process is shown in Fig. 1.

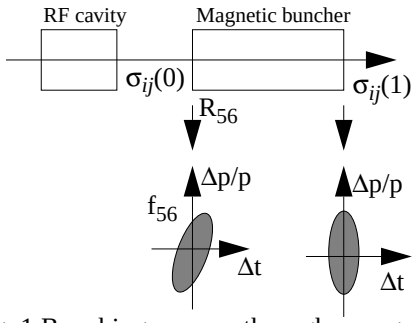

Fig. 1 Bunching process through a magnetic buncher

The bunch length after a magnetic buncher is

$$\sigma_{55}(1) = \sigma_{55}(0)\,(1 - R_{56}/f_{56})^2 + (R_{56}\varepsilon_z)^2/\sigma_{55}(0), \quad (7)$$

where $\varepsilon_z = \sqrt{\sigma_{55}(0)\sigma_{66}(0) - \sigma_{56}^2(0)}$ is the longitudinal emittance, and $f_{56} = -\sigma_{55}(0)/\sigma_{56}(0)$ measures the tilt of the longitudinal phase space distribution of the beam at the entrance of the magnetic buncher. The axial matching condition is $f_{56} = R_{56}$ [11,12] under which the bunch length is minimum. The intermediate emittance growth at the symmetry plane is related to the beam momentum spread introduced for matching R_{56} with f_{56} in the form of $\Delta\varepsilon_{nx} = (\eta_c/f_x)\,\sigma_{\gamma\beta}(0)\,\sigma_x(0)$, which can hardly be removed completely at the end of the magnetic buncher. Therefore, a balance must be struck between matching and minimizing the beam momentum spread to ease the emittance cancellation through the achromaticity of the system.

V. APPLICATION

The original injection line design for the proposed CEBAF UV FEL injector/accelerator is shown in Fig. 2.

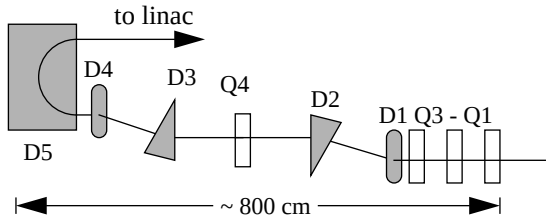

Fig. 2 The original 180°-bend injection line (R_{56} =0).

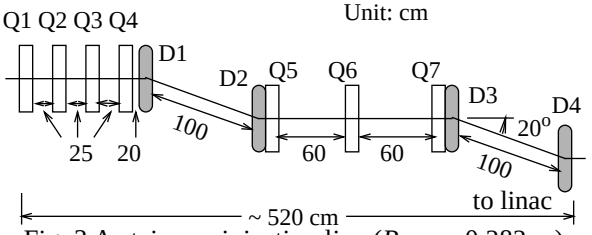

Fig. 3 A staircase injection line (R_{56} = –0.282 m).

A number of alternative designs have been investigated, two of which are shown in Figs. 3 and 4, to reduce the

beam emittance growth and to decouple the high-pass accelerated beams with the injected beams from that 180 degree bend. Fig. 3 is a staircase-line consisting of 7 quads and 4 parallel dipoles, and Fig. 4 is a slide-line consisting of 4 quads and 3 sector dipoles.

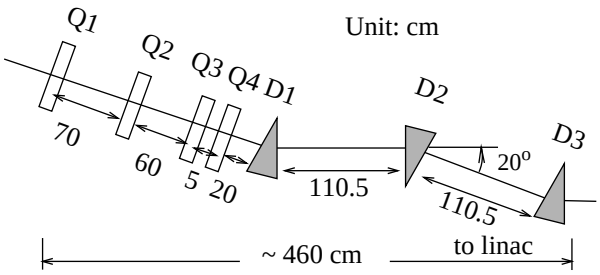

Fig. 4 A slide injection line (R_{56} = –0.138 m).

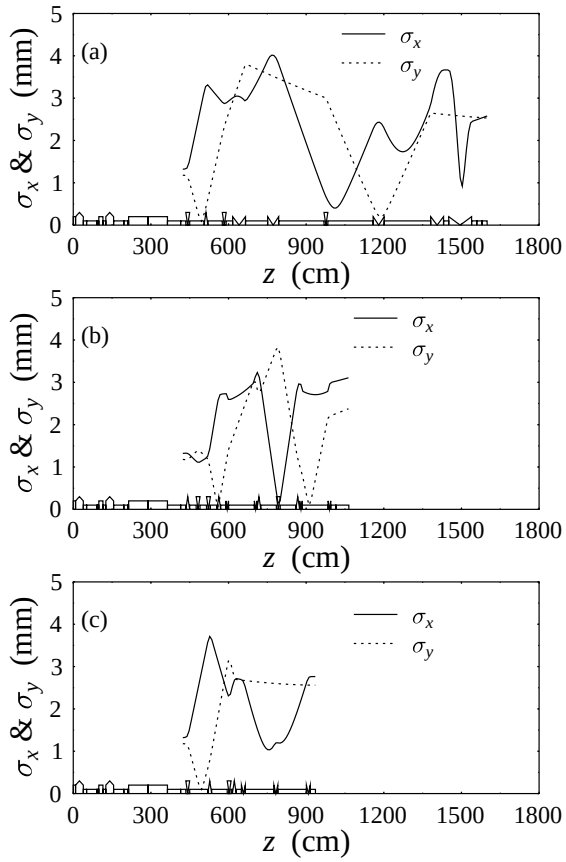

Fig. 5 Beam envelope evolution in three injection lines: (a) 180°-bend; (b) staircase; (c) slide.

Table 1 shows the performance comparisons among these three designs. The numbers in the table are the beam parameters at the end of each injection beam line.

Table 1 Performance comparisons among three designs

Beam parameters	180°-bend	staircase	slide
ε_{nrms} (π mm mrad)	8	6.8	4.6
$\varepsilon_{\phi rms}$(π keV-deg)	27	19	15
$4\sigma_t$ (ps)	11	10	4

The simulations started from the cathode with a 135 pCcharge/bunch, and continued to the cryounit exit, with theintermediate results saved. Then we restarted the simulation by incorporating each injection line with the preceding part. The restarted beam parameters are: transverse normalized emittance ε_{nrms} = 4.2 π mm mrad, longitudinal emittance $\varepsilon_{\phi rms}$ = 11.6 π keV-deg, and bunch length $4\sigma_t$ = 6.7 ps.

Fig. 5 shows the beam envelope evolution along these lines. It is seen that the beam's betatron-oscillation becomes more and more regular, and the number of cross-overs (very small beam waists) becomes smaller and smaller, from the 180°-bend-line to the slide-line. Due to its simplicity and better performance, the slide-design is chosen as the nominal injection beam line for the CEBAF FEL injector.

As is seen from Fig. 5 (c), the 4 quads before the three sector dipoles in the slide-line constitute a telescopic lens which can variably magnify the beam's β-functions from the cryounit exit to the entrance of the first dipole. The 3-magnet bending system preserves the beam's parallelness in both *x*- and *y*-plane [13, 14] while transporting the beam to the main accelerator. Betatron-function magnification and beam deflection are thus decoupled, which will greatly ease the operation.

Finally, we note that this 3-magnet bending system is non-isochronous with $R_{56} = \rho(3\alpha - 4\sin\alpha)$, where ρ and α are the bending radius and angle of each dipole. The achromaticity condition is $L/\rho = \cot\alpha - \tan(\alpha/2)$, where *L* is the edge-to-edge distance between the two adjacent dipoles. The dispersion at the symmetry plane is $\eta_c = \rho(2\cos(\alpha/2) - 1)$, and the focal length is $f_x = \rho/2\sin(\alpha/2)$. For small α's, we have $\eta_c/f_x \approx \alpha$, which reduces Eq. (5) to Eq. (11) of [9].

We wish to thank J. Bisognano, D. Douglas and B. Carlsten for discussions. This work was supported by the Virginia Center for Innovative Technology and DOE Contract # DE-AC05-84ER40150.

VI. REFERENCES

[1] D. Neuffer et al., these proceedings.
[2] F. Dylla et al., these proceedings.
[3] H. Liu et al., these proceedings.
[4] H. Liu et al., Nucl. Instr. Meth. **A358** (1995) 475.
[5] B. Carlsten et al., Nucl. Instr. Meth. **A296** (1992) 687.
[6] D. Douglas, private communication.
[7] R. Rand, *Recirculating Electron Accelerators,* (Harwood Academic Publishers, New York, 1984).
[8] H. Enge, Rev. Sci. Instrum., **34** (1963) 385.
[9] B. Carlsten et al., Phys. Rev. E. **51** (1995) 1453.
[10] A. Banford, *The Transport of Charged Particle Beams*, London, E. & F. N. Spon Limited, 1966.
[11] H. Liu, CEBAF TN# 95-004.
[12] T. Raubenheimer, Workshop on 4th Generation Light Sources, SSRL, (1992) 263.
[13] S. Penner, Rev. Sci. Instrum., **32**, 150 (1961).
[14] B. Milman, Nucl. Instrum. Methods, **20** (1963), p.13.